Journal of Micromechanics and Microengineering

# Characterization of carbon nanotube nanoswitches with gigahertz resonance frequency and low pull-in voltages using electrostatic force microscopy

To cite this article: Miao Lu *et al* 2010 *J. Micromech. Microeng.* **20** 105016

J. Micromech. Microeng. **20** (2010) 105016 (7pp) doi:10.1088/0960-1317/20/10/105016

# Characterization of carbon nanotube nanoswitches with gigahertz resonance frequency and low pull-in voltages using electrostatic force microscopy

**Miao Lu**[1], **Xuekun Lu**[2], **Min-Woo Jang**[2], **Stephen A Campbell**[2] **and Tianhong Cui**[1]

[1] Department of Mechanical Engineering, University of Minnesota, Minneapolis, MN, USA
[2] Department of Electrical and Computer Engineering, University of Minnesota, Minneapolis, MN, USA

E-mail: tcui@me.umn.edu

Received 24 March 2010, in final form 16 June 2010
Published 10 September 2010
Online at stacks.iop.org/JMM/20/105016

**Abstract**

An electrostatic force microscope (EFM) was used to characterize single-walled carbon nanotube (SWNT)-based nanoswitches in this paper. A conductive atomic force microscopy (AFM) tip acted as a mechanical probe as well as a positioning electrode in the experiment. The resonance frequency of the SWNT beams was computed from the measured SWNTs' dimension and spring constant. The pull-in voltages and the corresponding gaps were extracted simultaneously from a set of force curves at different EFM probe bias voltages. The adhesive force between the AFM tip and the SWNT beam was measured through the analysis of retract force curves. The relationship between the pull-in voltage and the SWNT nanoswitch gap was in agreement with the electrostatic pull-in theory. Long-range forces such as meniscus force or electrostatic force from surface charges engaged the SWNT beam when the gap was below 6 nm in atmosphere. The SWNT beam with a resonance frequency of 1.1 GHz was actuated by a voltage of 2 V for a gap of 6.5 nm. The average adhesive force between an SWNT beam and a platinum/iridium (PtIr5)-coated tip was found to be about 50 nN. Considering the stiffness of the 1.1 GHz SWNT beam, the elastic restoring force at 6.5 nm exceeds 53 nN, which will overcome the adhesive force and release the 1.1 GHz SWNT beam. Finally, some possible approaches to further improve the behavior of SWNT nanoswitches are discussed.

(Some figures in this article are in colour only in the electronic version)

## Introduction

Low pull-in voltage and high-frequency nanoswitches are very promising for low-power nanoelectronics, communication networks and random access memory technology. Nanoswitches working at a frequency in the GHz regime, driven at a CMOS compatible actuation voltage and integrated into a high-speed CMOS circuit, have been the target of many researchers [1]. Cantilever-based electrostatic switches have been widely studied due to their high speed and low actuation energy [2]. Theoretically, materials with a lower density may achieve nanoswitches with a high speed at a low pull-in voltage, because the low mass density of the cantilever leads to a fast switching speed for a given Young's modulus and dimensions of the nanoswitch. The high Young's modulus provides enough stiffness of cantilever beams at an actuation gap in the nanometer scale, which leads to a lower electrostatic pull-in voltage. Therefore, a single-walled carbon nanotube (SWNT) is one of the most promising materials for nanoswitches. Its density and Young's modulus are 1400 kg m$^{-3}$ and 1.2 TPa [3], about 60% and 7.5 times of polysilicon, respectively.

Suspended carbon nanotubes have been theoretically and experimentally investigated for switches in the GHz regime.

 

Kinaret *et al* modeled an SWNT nano-relay structure using a CNT of length 75 nm and diameter 2 nm, and predicted a pull-n voltage below 2 V, while the van der Waals force and adhesive force between the CNT and the substrate were neglected [4]. Campbell *et al* investigated an SWNT nanoswitch; the pull-in voltage of this fabricated device was about 5 V, and the length of the nanotube cantilever was approximately 2–2.5 $\mu$m, while the diameter spanned the range of 20–100 nm [5, 6]. Cruden and Cassell studied a vertically aligned CNT switch of about 10 $\mu$m length and 100 nm diameter, and the lowest pull-in voltage 3.7 V [7]. Cha *et al* presented a nanoswitch consisting of a suspended CNT of length 800 nm and diameter 20–40 nm, and a pair of self-aligned electrodes with a threshold voltage of 3.6 V for electromechanical switching [8]. Kaul *et al* described a chemical vapor deposited SWNT nanoswitch with a switching time down to a few nanoseconds, with a pull-in voltage of less than 5 V; the length of the suspended SWNT beam was about 250 nm and the diameter 2 nm [9]. On the other hand,Czaplewski *et al* reported a Ru metallic beam NEMS switch [10]. The operating voltage of the switch was approximately 13.2 V. The switch delay time was measured in less than 100 ns. Jang *et al* formed a switch with a TiN beam of 30 nm thickness and an air gap of 20 nm, the pull-in voltage was greater than 10 V, and the switching time was not measured [11]. The previous reports demonstrated the merits of CNT-based switches. However, the experimental results did not fully meet the requirements for nanoelectronics applications, while the theoretical results did not clarify the interactions between metal electrodes and SWNTs in a gap of several nanometers.

Atomic force microscopy (AFM) has been extensively used to characterize nanostructures and provides an effective way to measure dimensions and deformation with sub-nanometer resolution [12]. Electrostatic force microscopy (EFM), as one type of AFM, has been adopted to investigate dc electrostatic nanoparticle manipulation [13] and electric charges of CNTs [14]. In this work, EFM was employed to simulate the pull-in and release process of SWNT switches in a variable nanoscale gap. The results are helpful to further study and improve the performance of SWNT nanoswitches.

This paper provides a generic approach using EFM to systematically follow and investigate SWNT nanoswitches. A nanoswitch structure was constructed with an SWNT beam suspended between two metal electrodes, and an electrically biased AFM tip was moved to approach the beam. The tip-to-beam separation allowed a continuously variable gap. The conductive AFM tip acted as a moving gate of the nanoswitch. The pull-in effect of the nanoswitch was characterized at different gaps and voltages, and the adhesive force was also measured through the retracting force curve. Accordingly, the minimized gap of a working switch, as well as the minimum pull-in voltage, can be obtained by comparing the adhesive force with the mechanical restoring force of the SWNT beam.

## Sample preparation

Dielectrophoretic self-assembly was used to fabricate suspended SWNT beams in this research. First, 20 nm thick chromium and 100 nm thick gold were deposited and patterned on a silicon dioxide surface, followed by a layer-by-layer (LbL) self-assembly of two bi-layers of poly(diallyldiamine chloride) (PDDA) and poly(styrene sulfonate) (PSS) and a layer of PDDA, making the surface positively charged. Because the uniformly positive charged surface is helpful for negative charged SWNT deposition, the repeatability of producing uniform samples was improved with the PDDA/PSS treatment. Next, a focused ion beam system (FEI Quanta 200 3D) was used to reduce gaps' width from 200 nm to 1.0 $\mu$m for two counter electrodes. The working conditions for this reduction were 30 keV and 50 nA. An SWNT (99% purified) water solution from Nanointegris with a concentration of 50 $\mu$g ml$^{-1}$ was put in an ultrasonic bath (80 W, 40 kHz). The chip was vertically immersed in the SWNT solution with an ac electric field across the two electrodes of 2 V $\mu$m$^{-1}$ and 5 MHz applied for 10 s. A schematic of the specimen structure and an SEM image are shown in figure 1. Here a bundle of SWNTs realizes a beam across two electrodes.

(*a*)

(*b*)

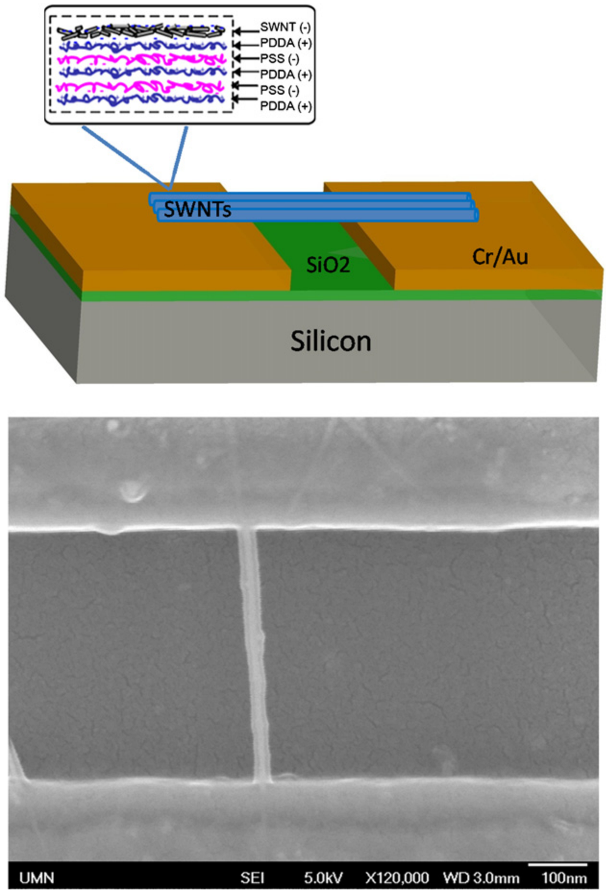


**Figure 1.** Schematic and SEM images of an SWNT beam sample: (*a*) two bi-layers of PDDA/PSS and a layer of PDDA were self-assembled to make the top surface positive charged. Next, SWNTs were assembled by a dielectrophretic process between two counter electrodes. (*b*) SEM image of the suspended SWNT bundle.

## Dimensions and mechanical properties

An AFM (Digital Instruments Nanoscope III Multimode) and a conductive AFM tip (PointProbe® Plus EFM, 25 nm thick

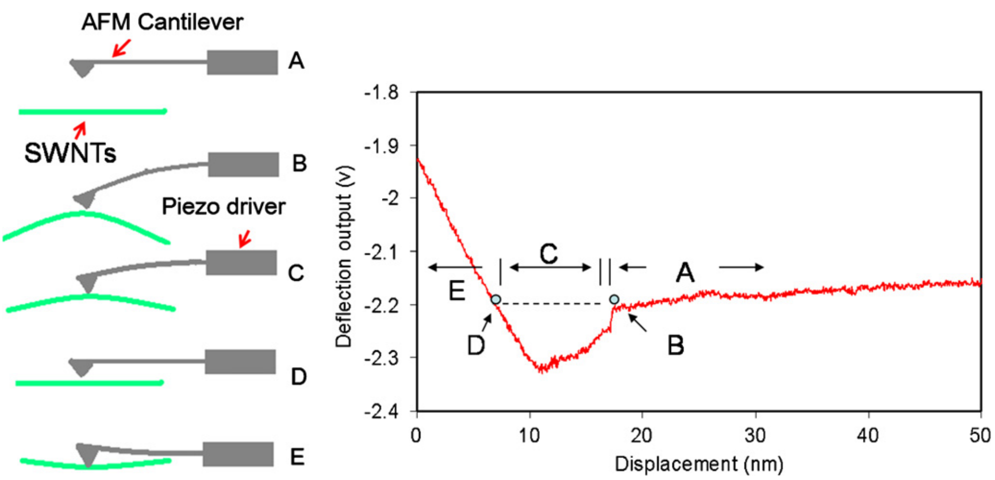


**Figure 2.** Five steps in the force plotting process between the SWNT beam and the EFM tip.

double layers of chromium and PtIr5 coating, nanosensors) were employed to measure the dimensions of the SWNT beams. The AFM worked on a tapping mode to snap images of SWNT beams, and the radius and length of the SWNT beams are computed from the imaging data.

The spring constant of an AFM cantilever was calibrated by a standard cantilever (CLFC-NOBO tipless calibration cantilevers, Veeco) to be 3.86 N $m^{-1}$. The spring constant of an SWNT beam can be measured by comparing the force curve on an SWNT beam with that on a solid surface. The AFM tip was driven to touch a solid surface and the center of the SWNT beam separately, and two different force plots were obtained due to the difference in the hardness of the two materials. The spring constant of SWNT beams can be calculated by the following equation [15]:

$$K_{\mathrm{SWNT}} = \frac{K_{\mathrm{AFM}}}{S_{\mathrm{solidsurface}}/S_{\mathrm{SWNT}} - 1} \tag{1}$$

where $S_{\mathrm{solidsurface}}$ and $S_{\mathrm{SWNT}}$ are the slope of the force curve on a solid surface and that on an SWNT beam, respectively. The resonance frequency of SWNT beams can be obtained from the following equation:

$$f = \frac{1}{2\pi}\sqrt{\frac{K_{\mathrm{SWNT}}}{\rho \times \pi \times r^2 \times l}} \tag{2}$$

where the SWNT beam is treated as a cylinder, $\rho$ is the mass density of the SWNT, $r$ and $l$ are the radius and the length of SWNT beams, respectively. In equation (2), $r$, $l$, $K_{\mathrm{SWNT}}$ are measured by AFM, and different mass densities of the SWNT were reported in the literature. The mass density of a single SWNT is 1400 kg $m^{-3}$ [3], the mass density of a bundle of SWNTs is about 1330 kg $m^{-3}$ [16], while the mass density of an 'SWNT forest' varies from 29 to 780 kg $m^{-3}$ [17]. In this experiment, the SWNT bundles formed by dielectrophoresis is believed to be packed together tightly due to the strong electric force, and a higher mass density leads to a lower estimated frequency in equation (2). Therefore, we used the mass density of 1400 kg $m^{-3}$ in this paper.

## Pull-in process characterization

In the EFM test, both electrodes on the sample were grounded through the scanner of the AFM, and the conductive AFM tip was biased by the system's embedded voltage source. First, the AFM was operated in a tapping mode to get images of the sample, and zoomed in at the central part of the SWNT beam. Next, the tapping mode operation was terminated by decreasing the tapping amplitude to zero, and the tip was biased. Force curves were plotted in a timely manner to ensure a negligible piezoelectric shift.

The force plotting process is shown in figure 2. The approach process can be divided into five steps: the tip and the SWNT beam were kept separate in step A; the pull-in voltage made the AFM cantilever bend down and the SWNT beam bend up, and contact with each other occurred at point B. The AFM cantilever moved down and continued to bend down by the restoring force of the SWNT beams in step C; the AFM cantilever and the SWNT beam return flat at point D; the AFM cantilever bent up and the SWNTs bent down as the AFM tip continued to move down in step E.

The gap between points B and D is recorded through a precise digital piezoelectric scanner. Four thousand ninety-six pixels were recorded in a range of 50 nm in the experiment, providing a resolution below 100 pm. The error of the pull-in gap is assumed to be about 100 pm because the force curves were plotted in a few seconds, and the piezoelectric hysteresis is negligible. Ideally, the pull-in voltage is the bias at this gap.

However, this model is different from an actual nanoswitch because both the AFM cantilever and the SWNT beam are deformed by the pull-in voltage, resulting in a bigger pull-in gap. The pull-in gap at which the SWNT beam is pulled in by a rigid electrode can be determined by a mechanical conversion. The model is shown in figure 3. The effective spring constant $K_{\mathrm{eff}}$ is given by

$$K_{\mathrm{eff}} = \frac{K_{\mathrm{SWNT}} \times K_{\mathrm{AFM}}}{K_{\mathrm{SWNT}} + K_{\mathrm{AFM}}} \tag{3}$$

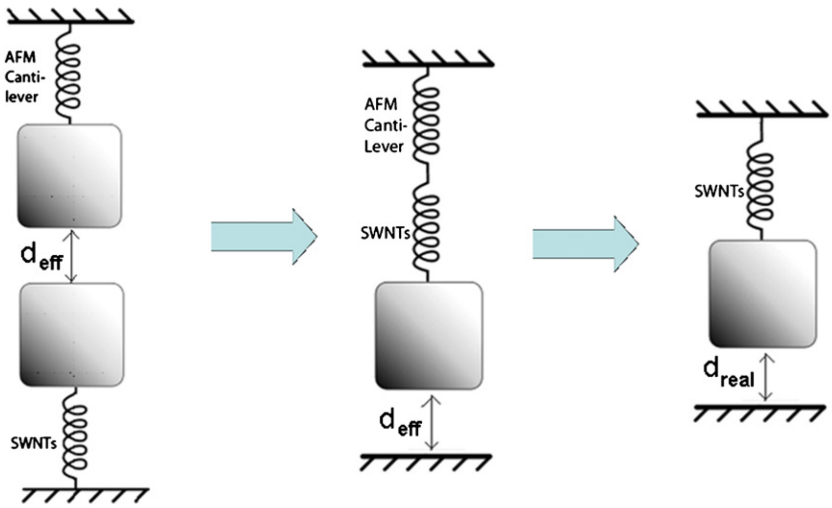


**Figure 3.** Illustration of the mechanical conversion model of the effective pull-in gap.

where $K_{SWNT}$ and $K_{AFM}$ are the spring constant of the SWNT beam and the AFM cantilever, respectively. In general, the pull-in voltage $V_{PI}$ is given by [18]

$$V_{PI} = \sqrt{\frac{8K_{eff}d_{eff}^3}{27\varepsilon_0 A_{eff}}} \tag{4}$$

where $\varepsilon_0$ is the permittivity of free space. In our experiments, the diameter of the SWNT beam is about 20–30 nm and that of the AFM tip is about 25 nm. The switch is modeled as a cylinder contact with a hemisphere. The governing equations for a cylindrical switch are given by Dequesnes *et al* [19] and Cruden *et al* [7]. However, it is hard to come up with an analytical solution. In the meantime, the pull-in gap between the tip and the SWNT bundle is measured by force curves in this experiment; the gap itself is an average result. Therefore, we use the basic pull-in formula and define $d_{eff}$ as the average gap and $A_{eff}$ as the average area of the equivalent capacitance to finish the mechanical conversion. $d_{real}$ replaces the 'real' pull-in gap in a 'real' nanoswitch gap for the same pull-in voltage given by

$$V_{pI} = \sqrt{\frac{8K_{SWNT}d_{real}^3}{27\varepsilon_0 A_{eff}}}. \tag{5}$$

From equations (3)–(5), the real nanoswitch gap can be deduced into the following equation:

$$d_{real} = \sqrt[3]{\frac{K_{AFM}d_{eff}^3}{K_{AFM} + K_{SWNT}}}. \tag{6}$$

The bias on the AFM tip varies from 0 to 7 V in this experiment, and force curves at each bias are recorded. The 'real' pull-in gaps are computed from the force curves and the relation between the pull-in voltage and the pull-in gap is identified.

## Adhesive force measurement

The nanoswitch cannot work continuously if the adhesive force is larger than the mechanical restoring force, unless an additional pull-out force is applied by more complex switch structures. The adhesive force of an SWNT beam and an AFM tip can be measured by the retracting curve of AFM force plotting [20, 21]. In this experiment, the force curves were plotted on the surface of gold and SWNT beam, respectively. The adhesive force was calculated by the following equation:

$$F_{adhesive} = \frac{\delta \times K_{AFM}}{S} \tag{7}$$

where $\delta$ is the difference between the deflection before and after contact, $S$ is the slope of the retracting force curve, $K_{AFM}$ is the spring constant of the AFM cantilever.

## Results and discussions

Samples with different dimensions were tested using the above method. The results of a sample are shown in figure 4. The diameter of the SWNT beam is measured to be 27 nm, and the length is 230 nm. The spring constant of the SWNTs is computed to be 8.1 N m$^{-1}$ from equation (1). The resonance frequency of the SWNT beam is 1.1 GHz by putting the dimensions and the spring constant into equation (2). The force curves for biases between 0 and 7 V are also shown in figure 4.

The three-dimensional AFM image of the SWNT beam is shown upper-left panel of figure 4. The length of the SWNT beam was obtained by measuring the distance between the two ends of the beam. The AFM tip traveled across the SWNT beam and the heights in different locations on the beam are shown in the bottom-left panel of figure 4, the point where an abrupt transition occurs is the edge of the beam, and the height difference between the edge and the maximum height is the radius of the SWNT beam; hereby we treat the beam as a cylinder. The force curves on an SWNT bundle and on a rigid surface are shown in the upper-right panel; the slopes of the curves are 37.5 mV nm$^{-1}$ and 55.4 mV nm$^{-1}$. The AFM tip is biased from 0 V to 7 V, the force curves are shown in the bottom-right panel, and the pull-in gaps at different biases are measured from these curves.

Another SWNT bundle, 640 nm long and 25 nm in diameter, was tested, and the spring constant is 0.51 N m$^{-1}$

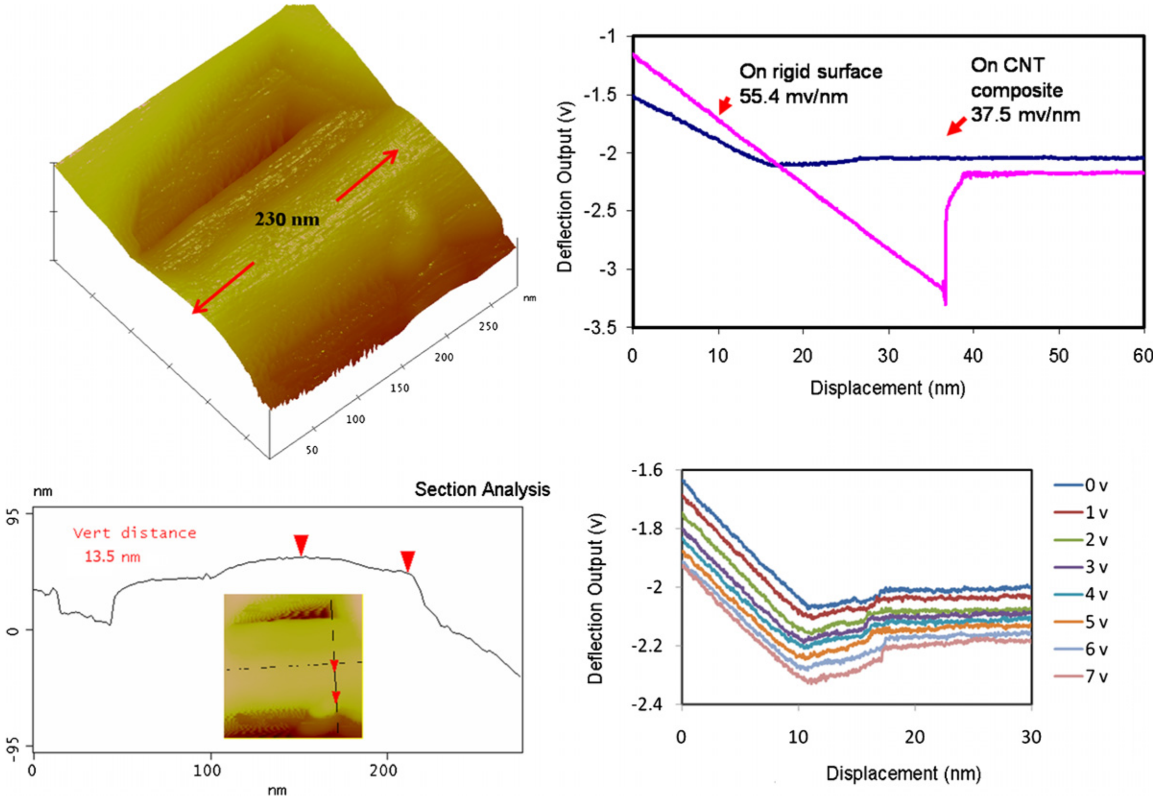


**Figure 4.** AFM testing results of sample I—left upper: measurement of the SWNT beam length; left bottom: measurement of the SWNT beam radius; right upper: force curves on a solid surface or at the center of the SWNT beam; right bottom: force curves at different biases of the AFM tip, the curves from top to bottom are biased from 0 to 7 V.

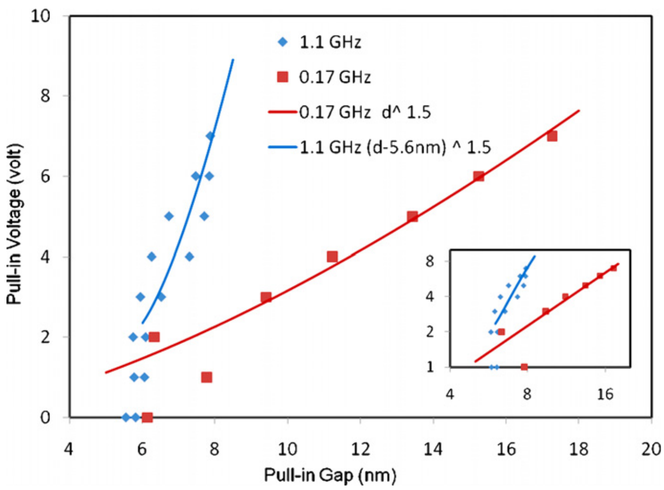


**Figure 5.** Relationship between the pull-in voltage and the pull-in gap of an SWNT beam.

from equation (1). The resonance frequency is calculated to be 0.17 GHz by equation (2).

The relationship between the pull-in voltage and the pull-in gap is shown in figure 5. The pull-in gap increases with the pull-in voltage at a bias larger than 2 V, and scatters below 2 V. At 0–2 V, the pull-in gap is near 6 nm, and the long-range forces, such as meniscus force and electrostatic force by surface charges, engaged the SWNT beam. Regarding meniscus force, because the AFM tests were implemented in atmosphere with a relative humidity, a thin layer of water was formed on the surface of the SWNT and AFM tip in this experiment. A liquid bridge, or a capillary neck, was formed when the tip approaches the SWNT beam in a critical gap, and the capillary produces a meniscus force to further engage the AFM tip and the SWNT beam. He *et al* investigated the liquid bridge in nanoasperity contacts using SFM [22]. Considering that the Lennard–Jones potential is proportional to the gap to a power of $-6$, van der Waals force is not likely to engage the SWNT bundle at a gap of 6 nm. After the SWNT beam is attracted into the range of less than 3 nm, van der Waals force will contribute significantly to the adhesive force [23], and the effect of applied voltages on the SWNT beams is not significant. These forces vary in different contacts to make the pull-in gap scattered, trend lines are added to analyze the relationship between the pull-in voltage and the gap. The pull-in voltage is proportional to the gap to the power of $3/2$ at the gap larger than 9 nm, as shown in the inset log plot in figure 5, which is in good agreement with the theoretical pull-in voltage in equation (4). The data at a gap below 6 nm are scattered due to the dominated long-range force. The data at a gap between 6 and 9 nm are proportional to the gap to the power of $3/2$, but the gap is subtracted by 5.6 nm. Hereby the SWNT beam will be pulled in if the electrostatic force reduces the gap to the active range of long-range forces, instead of the whole

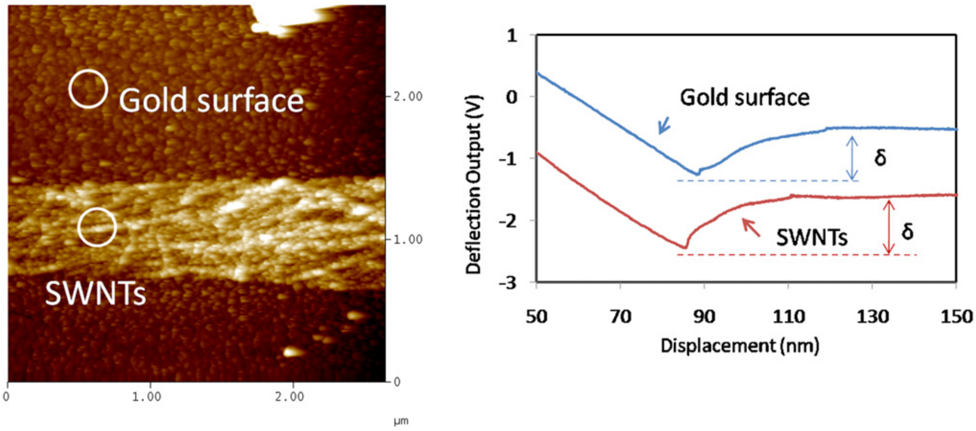


**Figure 6.** The adhesive force between the AFM tip and the SWNT beam; left: the locations of the force plotting in the AFM image; right: the retracting force curves on the gold surface and on an SWNT beam.

gap to a power of 3/2. If $d_{\mathrm{eff}}$ is replaced by ($d_{\mathrm{eff}}$–$d_{\mathrm{longrange}}$), equation (4) is given by

$$V_{\mathrm{PI}} = \sqrt{\frac{K_{\mathrm{eff}}(d_{\mathrm{eff}} - d_{\mathrm{longrange}})^3}{\varepsilon_0 A_{\mathrm{eff}}}} \tag{8}$$

where $d_{\mathrm{longrange}}$ is the gap at the long-range force engaged the SWNT beam, about 5.6 nm to get the best fit to the data.

The AFM image of an SWNT beam on a gold surface and the retracting force curves are shown in figure 6. Using equation (7), the adhesive force between the AFM tip and the SWNT film is calculated to be in the range from 40 nN to 60 nN with an average force of 50 nN, slightly more than the average adhesive force between the AFM tip and the gold surface, which is about 46 nN.

For the SWNT switch with 1.1 GHz resonance frequency, it is found that a pull-in voltage of 2.0 V corresponds to a pull-in gap of about 6.5 nm. Considering that the spring constant is about 8.1 N m$^{-1}$, the mechanical restore force at 6.5 nm exceeds 53 nN, larger than the average adhesive force between the tip and the SWNT beam (50 nN). It implies that SWNT nanoswitches with a working frequency of 1.1 GHz for a pull-in voltage of 2.0 V are feasible. Recently, an SWNT nanoswitch was fabricated using a similar dielectrophoretic self-assembly process by our group, and a switching time of 0.6 ns and a pull-in voltage of about 3.7 V were reported [24].

Several approaches to further improve the switching speed and reduce the pull-in voltage are discussed. First, the performance of SWNT nanoswitches can be further improved by increasing the effective actuation area according to equation (5). The increase of the effective actuation area will decrease the pull-in voltage if the contact area does not increase proportionally. Otherwise, the increasing adhesive force will cause stiction of the SWNT beam to the EFM tip. In addition, a rigid SWNT beam is necessary to make a big difference between the actuation area and the contact area because the rigid beam is hardly deformed to match the topographic contour of the contact electrode by the pull-in force, and keeps a smaller contact area.

Second, long-range forces, such as meniscus force or electrostatic force due to surface charges, may play an important role in the pull-in and release behaviors of the SWNT nanoswitches. If the gap is below 6 nm in air, the SWNT beam is engaged to the EFM tip (equivalent to the counter electrode), and cannot be released. This imposes a minimum working gap of nanoswitches operating in a normal atmosphere. Some approaches including humidity control, vacuum packaging and surface charge neutralization may be helpful in minimizing this gap limitation, resulting in a further decrease in the pull-in voltage of nanoswitches.

## Conclusions

This paper proves that when EFM is properly applied, it is an effective approach to characterize nanoscale beams and investigate the switching mechanism for nanoswitches without the necessity of complete fabrication of the entire nanoswitch structure. By this approach, it is demonstrated that SWNT beams with a resonance frequency of more than 1 GHz can be actuated by a low pull-in voltage. Some long-range forces such as meniscus force or electrostatic force due to surface charges may engage the SWNT beams when the gap is below 6 nm in a typical laboratory environment. The adhesive force between the AFM tip and the SWNT beam ranges from 40 to 60 nN. Further improvement in SWNT nanoswitches may be achieved by reducing these long-range forces and optimizing the effective actuation area.

## Acknowledgments

This work was partially supported by the DARPA NEMS Program. We also acknowledge the assistance by the Nanofabrication Center and Characterization Facility at the University of Minnesota, which are supported by NSF through NNIN. In particular, we thank Dr Greg Haugstad for the valuable discussion on AFM techniques.

## References

[1] Yousif M Y A, Lundgren P, Ghavanini F, Enoksson P and Bengtsson S 2008 CMOS considerations in

nanoelectromechanical carbon nanotube-based switches *Nanotechnology* **19** 285204
[2] Chakraborty R B, Narasimhan S and Bhunia S 2007 Hybridization of CMOS with CNT-based nano-electromechanical switch for low leakage and robust circuit design *IEEE Trans. Circuits Syst.* **54** 2480–8
[3] Collins P G and Avouris P 2000 Nanotubes for electronics *Sci. Am.* **283** 62–9
[4] Kinaret J M, Nord T and Viefers S 2003 A carbon-nanotube-based nanorelay *Appl. Phys. Lett.* **82** 1287–9
[5] Lee S W, Lee D S, Morjan R E, Jhang S H, Sveningsson M, Nerushev O A, Park Y W and Campbell E E B 2004 A three-terminal carbon nanorelay *Nano Lett.* **4** 2027–30
[6] Axelsson S, Campbell E E B, Jonsson L M, Kinaret J, Lee S W, Park Y W and Sveningsson M 2005 Theoretical and experimental investigations of three-terminal carbon nanotube relays *New J. Phys.* **7** 245
[7] Cruden B A and Cassell A M 2006 Vertically oriented carbon nanofiber based nanoelectromechanical switch *IEEE Trans. Nanotechnol.* **5** 350–5
[8] Cha S N, Jang J E, Choi Y and Amaratung G A J 2005 Fabrication of a nanoelectromechanical switch using a suspended carbon nanotube *Appl. Phys. Lett.* **86** 083105
[9] Kaul A B, Wong E W, Epp L and Hunt B D 2006 Electromechanical carbon nanotube switches for high-frequency applications *Nano Lett.* **6** 942–7
[10] Czaplewski D A, Kraus G M and Nordquist C D 2009 Nanomechanical switches for power saving in CMOS application *Electron. Lett.* **45** 550–1
[11] Jang W W *et al* 2008 NEMS switch with 30 nm-thick beam and 20 nm-thick air-gap for high density non-volatile memory applications *Solid-State Electron.* **52** 1578–83
[12] Yacoot A and Koenders L 2008 Aspects of scanning force microscope probes and their effects on dimensional measurement *J. Phys. D: Appl. Phys.* **41** 103001
[13] Toset J, Casuso I, Samitier J and Gomila G 2007 Deflection–voltage curve modeling in atomic force microscopy and its use in DC electrostatic manipulation of gold nanoparticles *Nanotechnology* **18** 15503
[14] Wang Z, Zdrojek M, Melin T and Devel M 2008 Electric charge enhancements in carbon nanotubes: theory and experiments *Phys. Rev.* B **78** 085425
[15] Cumpson P J, Hedley J and Zhdan P 2003 Accurate force measurement in the atomic force microscope: a microfabricated array of reference springs for easy cantilever calibration *Nanotechnology* **14** 918–24
[16] Gao G, Çagin T and Goddard W A III 1998 Energetics, structure, mechanical and vibrational properties of single-walled carbon nanotubes *Nanotechnology* **9** 184–91
[17] Futaba D N, Hata K, Yamada T, Hiraoka T, Hayamizu Y, Kakudate Y, Tanaike O, Hatori H, Yumura M and Iijima S 2006 Shape-engineerable and highly densely packed single-walled carbon nanotubes and their application as super-capacitor electrodes *Nature Mater.* **5** 987–94
[18] Huang J M, Liew K M, Wong C H, Rajendran S, Tan M J and Liu A Q 2001 Mechanical design and optimization of capacitive micromachined switch *Sensors Actuators* A **93** 273–85
[19] Dequesnes M, Rorkin S V and Aluru N R 2002 Calculation of pull-in voltages for carbon-nanotube-based nanoelectromechanical switches *Nanotechnology* **13** 120–31
[20] Poggi M A, Bottomley L A and Lillehei P T 2004 Measuring the adhesion forces between Alkanethiol-modified AFM cantilevers and single walled carbon nanotubes *Nano Lett.* **4** 61–4
[21] McElroy K, Davis R C and Hawkins A 2007 The effect of contact length on adhesion between carbon nanotubes on silicon dioxide *Appl. Phys. Lett.* **91** 233119
[22] He M Y, Blum A S, Aston D E, Buenviaje C and Overney R M 2001 Critical phenomena of water bridges in nanoasperity contacts *J. Chem. Phys.* **14** 1355–60
[23] Ashino M, Schwarz A, Behnke T and Wiesendanger R 2004 Atomic-resolution dynamic force microscopy and spectroscopy of a single-walled carbon nanotube: characterization of interatomic van der Waals forces *Phys. Rev. Lett.* **93** 136101
[24] Jang M W, Lu M, Cui T and Campbell S A 2009 Functional 1.6 GHz MEMS switch using aligned composite CNT membrane by dielectrophoretic self-assembly *Proc. Solid-State Sensors, Actuators and Microsystems Conf. (Transducers 2009) (Denver, CO, 21–25 June 2009)* pp 912–5